

# Corrosion Behavior of Magnesium Implants Coated with Biocomposite Polymer

Zainab F. Al-Sherify<sup>1, a)</sup>, Nawal Mohammed Dawood<sup>2, b)</sup> and Zuheir Talib Khulief<sup>3, c)</sup>

<sup>1,2,3</sup> *College of Materials Engineering/ Metallurgical Engineering department, University of Babylon*

## Abstract

Mg and its alloys consider as biodegradable metal with improve mechanical qualities and corrosion resistances. The rate of degradation of AZ31 Mg alloy as temporary implants is investigated in this work. the spin coating technique used to evaluate the effect of biocompatible polymer coating (polymethylmethacrylate PMMA) and composite coating (PMMA/hydroxyapatite (HA)) on the degradation rate of AZ31 magnesium. Some experiments were achieved to estimate the performance of coating. Such as AFM, FESEM, contact angle (CA), hydrogen evolution, simple immersion test to show the change of solution pH with time potentiostatic polarization. The results show a difference in the surface roughness and surface topography of the specimens that coated with composite coating in different concentrations. The second coating layer covering any cracks or pores if it found in the first coating layer. The thickness of the single polymer coating is much higher than the thickness of all composite polymer coatings. From potentiostatic polarization can show the coating efficiency (E%) of single PMMA coated specimens in 0.9%NaCl solution are around 97.41% for B specimen to 92.24% for C specimen compared with 99.28 and 99.23% for specimen coated with one and two layers of PMMA/7.5%HA composite coating, respectively, indicating a much lower corrosion rate and the best corrosion resistance. During the total immersion period of 45 days, the change in the pH values of the immersion solution containing coating specimen was fairly stable and significantly lower than that of the bare specimen, a general tendency can be seen, with an initial increase in the pH value as degradation started, followed by a draw towards saturation after a few days.

*Keywords. Biocomposite coating, biodegradable implant, AZ31 Mg alloy, spin coating;*

## 1.Introduction

The concept of biodegradable materials is as basic as that; some implant may only be required for a limited time to aid in the repair of sick tissue. These temporary implants are expected to be used in a variety of cases, including cardiovascular, orthopedic, and pediatric fields [1]. In other word, biodegradable metals are designed to provide a temporary support to the damaged tissues until the healing process was complete and then it is gradually dissolved. It has two primary characteristics: temporary support and decay. During the healing process, degradable metals are also predicted to interact favorably (bioactively). The degrading metals and their products aren't supposed to interfere with the healing process [2]. Biodegradable metals such as zinc (Zn), iron (Fe) and magnesium (Mg) have attracted the attentions of biomedical researchers [1]. Two surgeries were needed for patients with bone fracture fixation, one for implantation and the other to remove the implant after it had healed. It raises patients' economic burden as well as their pain [3]. Therefore, it is sometimes preferable to use biodegradable materials [4].

Magnesium alloys are very attractive material for structural components due to their excellent strength/weight ratios. At present time, Mg alloys are commonly used in the automotive industry, but their biocompatibility and biodegradability also provide possibilities for biomedical applications, such as degradable stents or bone fracture fixation pins [5,6]. The relation between degradable materials and body reactions is complex and difficult; the decomposition process or corrosion products can cause inflammatory responses, and the inflammatory products can then accelerate the degradation process [7]. Even pharmaceutical that the patient receives affect the corrosion process, since, to avoid the rapid decomposition of Mg, it has been suggested that acid nutrients or diluted hydrochloric acid be taken orally [8].

The extremely very bad corrosion resistance of the magnesium and its alloys can be mostly attributes to two key factors. The first one, the extremely electronegative potential of magnesium which cause proceed the corrosion even in oxygen absences, at such a negative potential, the cathodic water reduction reaction takes precedence. The second one, a weak protection property of any film form upon magnesium surface. This mean that any oxide or hydroxide layers that formed upon magnesium surface will be soluble in the most aqueous environments or in the humidity presence. Moreover, the Mg surface layer cover the underlying Mg metal incompletely and is highly defective [9]. The corrosion mechanisms must be decreased and regulated in order for Mg alloys to be suitable for orthopedic applications. Because Mg alloying is difficult due to the low solubility of several elements in Mg, the development of coatings on Mg alloys is important and could be an appealing way to improve corrosion resistance. Coatings protect a substrate by forming a barrier between the metal and the corrosion environments. Coatings must be homogeneous and adhered effectively to provide adequate corrosion protection [10].

The aim of present work is to decrease the magnesium implants degradation rate in the living body until healing process complete by using a biodegradable coating, this was accomplished by investigating the degradation rate of AZ31 magnesium alloy as a temporary implant in 0.9% NaCl solution and the effects of a biocompatible polymer coating (polymethylmethacrylate PMMA) on the surface of AZ31 alloy on the degradation rate of AZ31 magnesium using the spin coating technique. In addition, using the spin coating process, study the effect of a composite coating (hydroxyapatite particles with PMMA) on the rates of degradation of AZ31 magnesium on the surface of the alloy.

## 2. Experimental works

### 2.1. Substrate Specimen

Small examples with a 12.5mm diameter were cut from a rolling plate constructed of AZ31 Mg alloy. The magnesium specimens were polished (from P180 to P400 grits) with silicon carbide (SiC) sheets, then washing in the ethanol and dried with hot air. Optical microscopy type optical microscopy was used to analyze the microstructure of AZ31 at a magnification of 800x (280 XEQ- MM 300 TUSB). Non-equiaxed and fine grains with twinning as a result of rolling the plate may be seen in the optical microscope pictures displayed in Fig. 1.

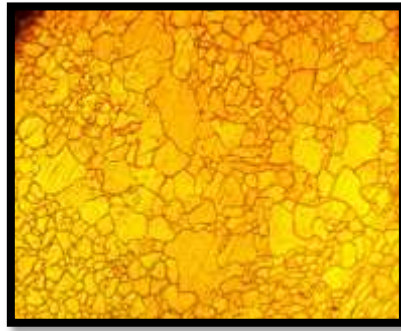


Fig. 1. AZ31 optical micrograph with 800X magnification.

### 2.2. Preparation of the coating

After dissolving 1g of PMMA in 20ml of chloroform at room temperature and stirring for only half an hour, it was employed as a coating material. To make the composite coating solution, different amounts of HA particles were dispersing in 20 ml of chloroform and stirred for two hours with a magnetic stirrer to eliminate any agglomeration in the powder and to ensuring that the particles were uniformly spread. Then, a little amounts of PMMA polymer was added to the dispersed the ceramic particles in the solvent and stirred for another half hour, until all of the PMMA grains were dissolved. Bioactive ceramic particles (HA) have been added to the polymeric covering in various percentages 2.5, 5 and 7.5 percent.

### 2.3. Spin Coating

The vacuum spin coater VTC-100 was used for the spin-coating process, which was carried out at room temperature. Specimens with a diameter of 12.5 mm were spun at a particular speed (2500 rpm) for 60 seconds after a coating solution of 0.1 mL was applied to the surface of an AZ31 Mg alloy substrate. After the coating technique, all coated Mg specimens were dried promptly; nevertheless, the coated specimens were stored under clean circumstances for further 20 hours at room temperature. To generate a sufficiently rough surface for good coating adherence, all specimens needing coating were ground with silicon carbide paper of 400 grades. All specimens were washed with ethanol using a sonication path before to the coating process, then dried with hot air before being baked in a 50°C oven. After multiple tests, both the spin time and the rotating velocity were chosen until we had a homogeneous coating layer with no segregation or agglomeration. The symbol code and description of several coated and uncoated AZ31 specimens are shown in Table 1.

Table 1. The symbols of the coated and uncoated Mg samples.

Specimens Symbols	Description
A	Bare AZ31
B	AZ31 with monolayer PMMA coating
C	AZ31 with bilayer PMMA coating
D	AZ31 with monolayer PMMA/2.5% HA coating
E	AZ31 with bilayer PMMA/2.5 %HA coating
F	AZ31 with monolayer PMMA/5 %HA coating
G	AZ31 with bilayer PMMA/5% HA coating
H	AZ31 with monolayer PMMA/7.5 %HA coating
I	AZ31 with bilayer PMMA/7.5 %HA coating

### 2.4. Characterization of The Coating

Several tests have been conducted, such as FESEM, AFM and contact angle, must be performed in order to demonstrate the characterisation of polymer coatings with and without HA particles. Micrographs taken with an Atomic Force Microscope (AFM) “Digital Instruments, CSPM-AA3000” were used to examine the surface roughness and topography of the specimens after thin film deposition, as well as the particle distribution on the coated specimens. MIRA 3-XMU Field Emission Scanning Electron Microscope was used to examine the surface morphology of the coated specimens (FESEM). The wettability was then measured using a contact angle device “Powreach, ST200KS, China”.

## 2.5. degradation evaluating

Mg samples were examined in 0.9%NaCl solution as electrolyte before and after coating. Three approaches were used to determine the corrosion behavior of the bare and coated Mg specimens: hydrogen evolution, Tafel extrapolation, and pH monitoring. The corrosion rate was calculated using the Tafel extrapolation method. In this cell, there were three electrodes: the working electrode represented the specimen, the counter electrode represented the platinum electrode, and the reference electrode represented the Ag/AgCl electrode. At the start of the specimen test, the voltage of each sample was read in open circuit. The open circuit potential value was being scanned at a rate of  $\pm 600$ . The instrument utilized was a "type DY2300" potentiostatic instrument. The corrosion rate (mm/year) can be calculated using the results from this test according to "ASTM G102" [11]:

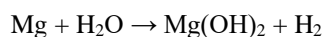
$$\text{corrosion rate} = K * i_{\text{corr}} * \frac{EW}{D} \quad \dots \dots \dots \text{Eq. 1}$$

Where:  $K = 3.27 * 10^{-3}$  mm.g/ $\mu\text{A}$ .cm.year,  $EW$  = Equivalent Weight,  $D$  = magnesium density ( $\text{g}/\text{cm}^3$ ), and  $i_{\text{corr}}$  = corrosion current density ( $\mu \frac{\text{A}}{\text{cm}^2}$ ).

$$i_{\text{corr}} = \frac{I_{\text{corr}}}{A} \quad \dots \dots \dots \text{Eq. 2}$$

Where:  $I_{\text{corr}}$  is the corrosion current ( $\mu\text{A}$ ), and  $A$  is the surface area of the specimen ( $\text{cm}^2$ ).

Hydrogen ( $\text{H}_2$ ) evolution was carried out for AZ31 magnesium samples with and without coating. The samples was hanging in the solution and did not come into contact with any of the surfaces. The hydrogen evolution can be used to calculate the corrosion rate. By employing a water bath, the temperature of the solution can be controlled around 37 °C. The hydrogen evolution rate investigations were done with a simple set-up, which is schematically illustrated in Fig. 2. This apparatus is suited for collecting hydrogen evolution and is straightforward to set up and use. Magnesium reacts rapidly with a 0.9% NaCl solution to produce hydrogen gas and hydroxide, as shown in the reaction below [12]:



Accumulating the hydrogen gas that evolves and then determining its volume is really an indirect indication of magnesium degradability kinetics.

Specimens were immersed in 0.9%NaCl as electrolyte medium at  $37^\circ\text{C} \pm 1$  for 45 days to obtain the pH measurements. The pH of the immersion solution was measured with a pH meter "type Hannai". The solution's pH was considered as an indicate to corrosion, since, it changes with immersion time.

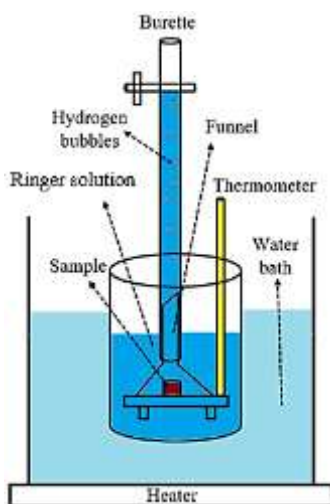


Fig.2: The setup for evaluating hydrogen evolution system.

## 3. Result and discussion

### 3.1 Coatings Characterizations

AFM and FESEM examinations were used to demonstrate morphology, surface roughness, layer thickness, and particle distributions. The coating layer thickness ( $\mu\text{m}$ ), surface roughness ( $R_a$ ) in nm, and contact angle (CA) of coating specimens are shown in Table 2.

Table 2: Coating Characterization coating layer thickness, surface roughness and contact angle values.

Specimen code	Coating thickness in $\mu\text{m}$	(Ra or Sc) in nm	CA in 0.9%NaCl
A			88.644
B	141.64	3.87	65.391
C	158.94	1.2	62.023
D	55.28	6.08	55.59
E	61.66	1.81	63.818
F	59.03	1.1	85.242
G	68.92	3.01	52.759
H	74.24	1.6	50.053
I	92.99	1.95	60.226

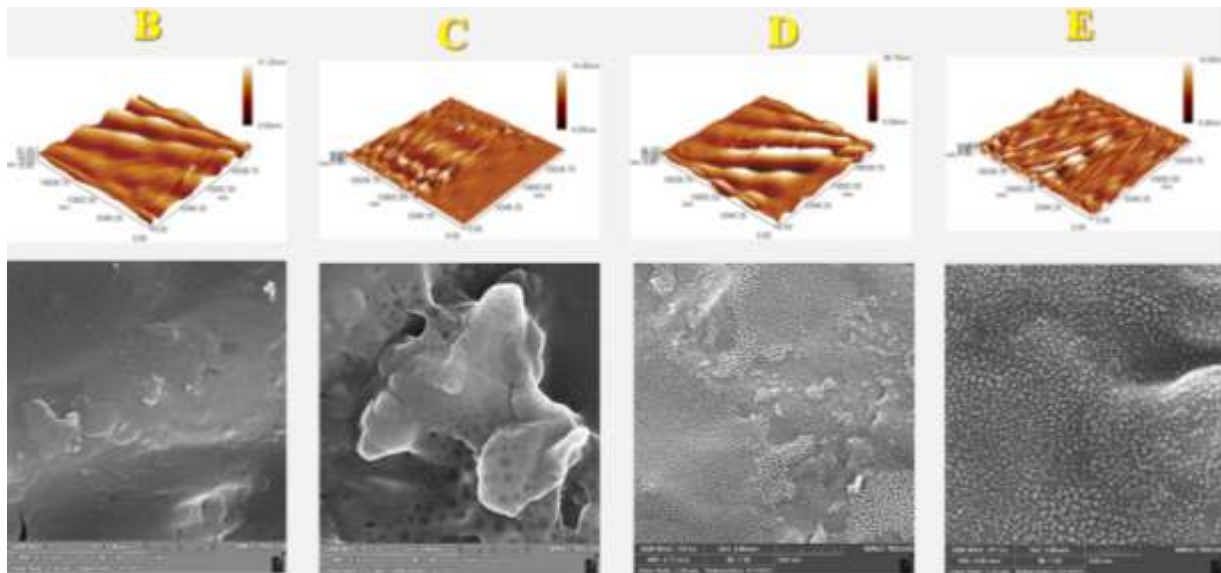
To assess the wettability of the surfaces with and without coating, contact angle test (CA) have been done. If the contact angles are between 0 and 90 degree, the surface has strong wettability and is classified as hydrophilic. If the contact angles are more than 90 degree, the surface is said to be hydrophobic.

Table 2 shows that the 0.9% NaCl contact angle reduces significantly from  $88.644^\circ$  on the uncoated specimen surface to  $50.053^\circ$  on the coated Mg alloy surface (H specimen). PMMA is a polymer that is hydrophilic. The improved hydrophilicity indicates that PMMA coated the magnesium surface effectively.

In general, we can see from table2 that all of the contact angle values for all coating specimens in 0.9 percent NaCl solution were less than 90, indicating that the coated specimens were hydrophilic. The CA of coated AZ31 was lower than that of AZ31 that had not been coated. The change in CA indicates that the coating has self-assembled on the surface. According to another studies [13,14], the adhering PMMA is hydrophilic, and the closing of pores and fissures is favorable to the spreading of water droplets, which could explain the lower CA on coated AZ31 surfaces.

Figure 3 shows 3D images of PMMA and PMMA with varying contents of HA composite coating with one and two layers taken from AFM and FESEM images. It can be seen that the surface topography of the sample covering surfaces differs slightly. The surface topography of the coated specimens shows the undulations created by the spinning of the specimen during coating. The spin coating resulted in a homogeneous dispersion of the bioceramics particles, as seen in the FESEM photos.

Any micro - cracks or micropores identified in the first coating layer were covered by the second coating layer. The coating's surface is smooth and homogeneous, and the coating entirely covers the Mg specimens, according to FESEM photos. The coating on the AZ31 sample was well covered, resulting in a thick layer on the surface, consistent with the result recorded in [15,16]. As can be seen in Fig. 3, the specimen B coated with one layer of PMMA polymer without a filler material has many microdefect like a micropores or microcracks caused by bubbles in the coating solution, but these eliminated when the sample covering with a bilayer of PMMA, as shown in the image of specimen C. Furthermore, the presence of faults in the second layer, such as bubbles, will be ineffective since the metal's surface will be covered by the first layer of coating, as shown in Fig. 3. (C). Also, we can see from the FESEM pictures that the HA particles dispersion is quite homogenous, with no agglomeration, which is owing to the coating process.



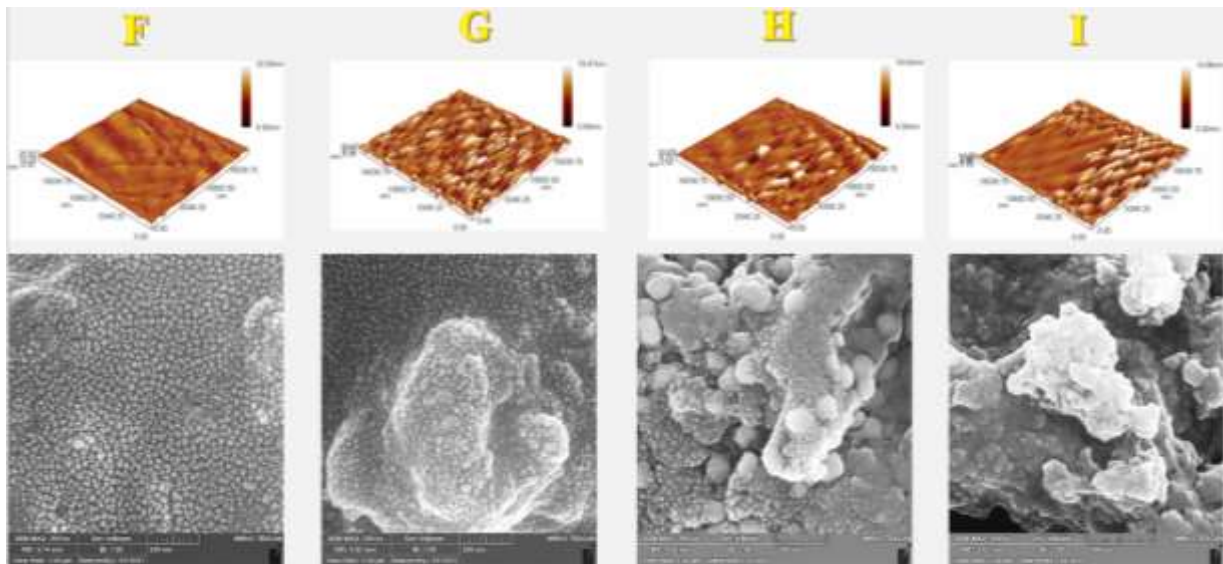


Fig. 3 . AFM and FESEM for different coatings.

### 3.2 Potentiostatic polarization test

The feasibility of measuring the corrosion parameters values such as corrosion current density ( $i_{corr}$ ), corrosion potential ( $E_{corr}$ ), and corrosion rate (CR) is clarified by the potentiostatic polarization test. In a 0.9 percent NaCl solution, Fig. 4 showed the Potentiostatic polarization curve of the coated and bare specimens, while table 3 showed the corrosion parameters which take from tafel curves, coating efficiency (E%), polarization resistance (Rp) and corrosion rate.

The covered specimens have a lower current density than the bare specimens, showing a strong decrease in corrosion rate, which is consistent with another researcher's observation [17]. A single PMMA coating on the surface of a magnesium alloy can be employed to generate a protective layer that prevents the diffusion of Mg ions [18]. As a result, as indicated in table 3, the current density and corrosion rate in 0.9 percent NaCl solution will drop. Figure 4 shows a significant shift toward lower current densities for PMMA/HA with varying percentages of HA coated samples; these findings are consistent with those of another researcher [19-23]. The corrosion current and determined corrosion rate are indicators of how much material is degraded during the corrosion reaction. As a result, more materials are lost due to the greater current density and predicted corrosion rate [24]. Polarization resistance (Rp) can calculate from the Stern-Geary [25-27]:

$$R_p = \frac{\beta_a \beta_c}{2.3 i_{corr} (\beta_a + \beta_c)}$$

where  $\beta_a$  represents the anodic Tafel slope,  $\beta_c$  represents the cathodic Tafel slope, while the  $i_{corr}$  represents the corrosion current density.

Table 3. Corrosion parameters taken from tafel curves in 0.9% NaCl.

Spec. code	$i_{corr}$	CR	$E_{corr}$	$\beta_a$	$\beta_c$	Rp	E%
A	2.22E-04	7.04E-04	-1501	4.00E+00	5.20E+00	4.43E+03	0.00%
B	6.35E-06	2.01E-05	-1236	7.36E+00	3.78E+00	1.71E+05	97.41%
C	9.55E-06	3.02E-05	-1303	1.44E+00	9.80E+00	5.70E+04	92.24%
D	2.78E-06	8.81E-06	-1555	9.04E+00	3.66E+00	4.07E+05	98.91%
E	7.47E-06	2.37E-05	-1164	4.28E+00	8.21E+00	1.64E+05	97.30%
F	2.16E-06	6.85E-06	-1344	7.31E+00	4.07E+00	5.26E+05	99.16%
G	2.05E-06	6.50E-06	-1516	8.51E+00	3.53E+00	5.28E+05	99.16%
H	1.59E-06	5.03E-06	-1453	8.81E+00	3.01E+00	6.15E+05	99.28%
I	1.97E-06	6.25E-06	-1408	8.25E+00	3.82E+00	5.76E+05	99.23%

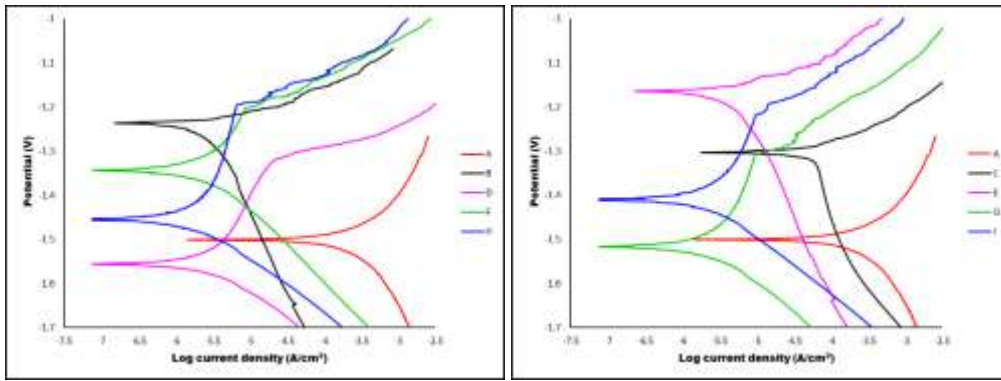


Fig. 4. Potentiostatic polarization in 0.9%NaCl solution for coated and uncoated specimens.

### 3.3 Hydrogen evolution

A relative long term corrosion behaviors of magnesium specimens can evaluate by hydrogen evolution experiment. Under an inverted burette system, hydrogen was collected by immersing the whole surface of the specimen in a 0.9 percent NaCl solution. The burette's solution level was measured at its highest point. Hydrogen gas evolution is noticed immediately after immersing of the AZ31 specimens in the solution, which is caused by magnesium corrosion [29-31].

The AZ31 alloy specimens, whether it is bare or coated with one or two layers of PMMA alone or PMMA with HA, were chosen as typical specimens and the hydrogen evolution from them in the immersion solution with a duration up to 45 days are illustrates in Fig.5. The uncoated AZ31 alloy released hydrogen quickly, as expected, while the coated specimens with single PMMA produced a lesser volume of hydrogen. In comparison to the naked AZ31 and single PMMA coating specimens, the specimens with PMMA composite coating provided greater substrate protection and produced less hydrogen. As a result of the breakdown of the magnesium substrate, hydrogen is released. It can be inferred that the AZ31 alloy degraded rapidly, especially during the first immersion stage, and that its corrosion rate slowed as time passed, which may be attributed to corrosion product generated on its surface. In addition, the corrosion rate of the PMMA coated specimens was lower than the uncoated Mg specimen. The AZ31 alloy that coated with PMMA/HA composite coating was the better protecting specimens, showing the lower volume of hydrogen gas. These findings are in line with those of other researchers [32].

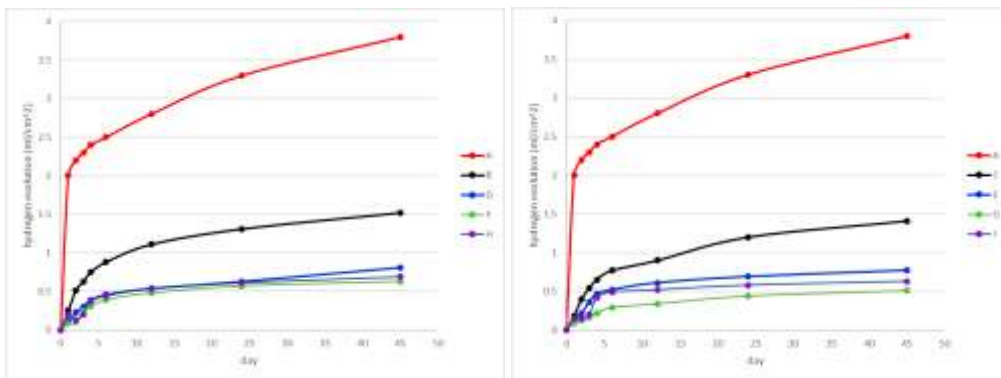


Fig. 5. Hydrogen-evolution in 0.9%NaCl solution of the coated and uncoated specimens.

### 3.4 pH-Measurement

The pH values were measured at corrosion medium after 1, 2, 3, 4, 6, 12, 24 and 45 days of immersion. The table 4 show the pH changes of 0.9%NaCl solution with time of immersion in days. It revealed that the immersion solution of all specimens resulting in an increased of pH solution values due to their alkaline corrosion product. A general trend can be seen, with an initial increased in the pH value as degradation progressed, followed by a draw towards saturation after a few days. All of the coatings gave excellent protection for the magnesium substrate comparing with the unprotected AZ31 alloy, especially during the first immersion period. So, when immersion time was increased, however, the coatings' protective efficiency differed significantly. The pH value variation of 0.9 percent NaCl solution containing coating specimens was comparatively continual and have a significant reduction than that of the uncoated AZ31 alloy during the 45-day test period.

Table 4. pH changes of 0.9%NaCl solution with time of immersion.

Time (day)	A	B	C	D	E	F	G	H	I
0	5.50	5.50	5.50	5.50	5.50	5.50	5.50	5.50	5.50
1	9.00	8.70	8.53	8.32	8.28	8.45	8.26	8.35	8.43
2	9.31	8.76	8.62	8.38	8.38	8.53	8.35	8.43	8.50
3	9.46	8.81	8.71	8.41	8.48	8.57	8.44	8.51	8.58
4	9.52	8.88	8.82	8.46	8.52	8.61	8.54	8.60	8.66
6	9.67	8.97	8.93	8.49	8.59	8.66	8.65	8.70	8.75
12	9.74	9.00	9.06	8.53	8.63	8.70	8.77	8.81	8.85
24	9.91	9.09	9.18	8.57	8.68	8.75	8.89	8.92	8.94
45	10.51	9.20	9.19	8.63	8.72	8.79	8.90	8.92	8.95

#### 4. Conclusion

Many of significant contributions to the corrosion research produce from this study and thus specified some conclusions. It can be note that the specimens coated with PMMA/HA composite coating and with different concentrations, have a coating thickness varies between 55.28 to 92.99  $\mu\text{m}$ . Also, can note that the thickness of the coating increases as the concentrations of ceramic particles increased, additionally to the increase in thickness when adding another coating layer of the same concentration. The corresponding Rp values of coating specimens were clearly increased more than of the bare AZ31. It represents that PMMA biocomposite coatings effective enhanced the corrosion protection to Mg alloy, better than that of single PMMA coatings. In general, as the immersion duration was extended, the corrosion area grew larger and the corrosion pits grew deeper. Finally, there was a lot of deterioration under the coatings. The results showed that the PMMA composite coating outperformed the single PMMA coating in terms of corrosion resistance, which was supported by electrochemical investigation. From the pH changes of 0.9%NaCl solution with time of immersion in days. It revealed that the immersion solution of all specimens resulting in an increased in the pH values. of the immersion solution due to their alkaline decomposition product. A significant enhancement was seen, with an initially increasing in pH as degradation progressed, followed by a draw towards saturation after a few days.

#### References

- [1] Park, J. B., & Bronzino, J. D. (2002). *Biomaterials: principles and applications*. crc press.
- [2] Logothetidis, S. (Ed.). (2012). *Nanostructured materials and their applications*. Springer Science & Business Media.
- [3] Zheng, Y. (2015). *Magnesium alloys as degradable biomaterials*.ss
- [4] Niinomi, M. (Ed.). (2019). *Metals for biomedical devices*. Woodhead publishing.
- [5] Krause, A., Von der Höh, N., Bormann, D., Krause, C., Bach, F. W., Windhagen, H., & Meyer-Lindenberg, A. (2010). Degradation behaviour and mechanical properties of magnesium implants in rabbit tibiae. *Journal of materials science*, 45(3), 624-632.
- [6] Witte, F., Fischer, J., Nellesen, J., Vogt, C., Vogt, J., Donath, T., & Beckmann, F. (2010). In vivo corrosion and corrosion protection of magnesium alloy LAE442. *Acta biomaterialia*, 6(5), 1792-1799.
- [7] Boutrand, J. P. (Ed.). (2019). *Biocompatibility and performance of medical devices*. Woodhead Publishing.
- [8] Witte, F. (2010). The history of biodegradable magnesium implants: a review. *Acta biomaterialia*, 6(5), 1680-1692.
- [9] Gusieva K, Davies CHJ, Scully JR, Birbilis N. Corrosion of magnesium alloys: the role of alloying. *Int Mater Rev* 2015;60:169-94.
- [10] Birbilis, N., Cain, T., Laird, J. S., Xia, X., Scully, J. R., & Hughes, A. E. (2015). Nuclear microprobe analysis for determination of element enrichment following magnesium dissolution. *ECS Electrochemistry Letters*, 4(10), C34.
- [11] Baboian, R. (Ed.). *Corrosion tests and standards: application and interpretation* (Vol. 20). ASTM international; 2005.
- [12] Salahshoor, M., & Guo, Y. B. Biodegradation control of magnesium-calcium biomaterial via adjusting surface integrity by synergistic cutting-burnishing. *Procedia CIRP*; 2014, 13, 143-149.
- [13] Trybała, A., Szyk-Warszyńska, L., & Warszyński, P. The effect of anchoring PEI layer on the build-up of polyelectrolyte multilayer films at homogeneous and heterogeneous surfaces. *Colloids and Surfaces A: Physicochemical and Engineering Aspects*; 2009, 343(1-3).
- [14] Wang, X., Yan, H., Hang, R., Shi, H., Wang, L., Ma, J., ... & Yao, X. Enhanced anticorrosive and antibacterial performances of silver nanoparticles/polyethyleneimine/MAO composite coating on magnesium alloys. *Journal of Materials Research and Technology*; 2021, 11, 2354-2364.

- [15] Boccaccini, A. R., Peters, C., Roether, J. A., Eifler, D., Misra, S. K., & Minay, E. J. Electrophoretic deposition of polyetheretherketone (PEEK) and PEEK/Bioglass® coatings on NiTi shape memory alloy wires. *Journal of materials science*; 2006, 41(24), 8152-8159.
- [16] Flamini, D. O., & Saidman, S. B. Electrodeposition of polypyrrole onto NiTi and the corrosion behaviour of the coated alloy. *Corrosion Science*; 2010, 52(1), 229-234.
- [17] Zomorodian, A., Garcia, M. P., e Silva, T. M., Fernandes, J. C. S., Fernandes, M. H., & Montemor, M. F. Corrosion resistance of a composite polymeric coating applied on biodegradable AZ31 magnesium alloy. *Acta biomaterialia*; 2013, 9(10), 8660-8670.
- [18] Rezk, A. I., Mousa, H. M., Lee, J., Park, C. H., & Kim, C. S. Composite PCL/HA/simvastatin electrospun nanofiber coating on biodegradable Mg alloy for orthopedic implant application. *Journal of Coatings Technology and Research*; 2019, 16(2), 477-489.
- [19] Akram, M., Arshad, N., Aktan, M. K., & Braem, A. Alternating Current Electrophoretic Deposition of Chitosan–Gelatin–Bioactive Glass on Mg–Si–Sr Alloy for Corrosion Protection. *ACS Applied Bio Materials*; 2020, 3(10), 7052-7060.
- [20] Loperena, A. P., Lehr, I. L., & Saidman, S. B. Improved Corrosion Resistance of AZ91D Mg Alloy by Cerium-Based Films. Formation of a Duplex Coating with Polypyrrole. *Russian Journal of Electrochemistry*; 2021, 57(1), 62-73.
- [21] Sasireka, A., Rajendran, R., & Raj, V. In vitro corrosion resistance and cytocompatibility of minerals substituted apatite/biopolymers duplex coatings on anodized Ti for orthopedic implant applications. *Arabian Journal of Chemistry*; 2020, 13(8), 6312-6326.
- [22] Wang, W., Yang, X. N., Wang, Y., Fan, Y., & Xu, J. N. Endowing magnesium with the corrosion-resistance property through cross-linking polymerized inorganic sol–gel coating. *RSC Advances*; 2021, 11(8), 4365-4372.
- [23] Singh, S., Singh, G., Bala, N., & Aggarwal, K. Characterization and preparation of Fe<sub>3</sub>O<sub>4</sub> nanoparticles loaded bioglass-chitosan nanocomposite coating on Mg alloy and in vitro bioactivity assessment. *International journal of biological macromolecules*; 2020, 151, 519-528.
- [24] Singh, R., & Dahotre, N. B. Corrosion degradation and prevention by surface modification of biometallic materials. *Journal of Materials Science: Materials in Medicine*; 2007, 18(5), 725-751.
- [25] Mansfeld, F. Fundamental aspects of the polarization resistance technique—the early days. *Journal of Solid State Electrochemistry*; 2009, 13(4), 515-520.
- [26] Delgado, M. C., García-Galvan, F. R., Barranco, V., & Batlle, S. F. A measuring approach to assess the corrosion rate of magnesium alloys using electrochemical impedance spectroscopy. *Magnesium Alloys*; 2017, 129-159.
- [27] Mena-Morcillo, E., Veleza, L., & Espadas-Herrera, L. J. Analysis of the degradation process and electrochemical behaviour of AZ31 magnesium alloy in artificial saliva. *Revista de Metalurgia*; 2020, 56(2), e166.
- [28] Song, G., Atrens, A., & StJohn, D. (2016). An hydrogen evolution method for the estimation of the corrosion rate of magnesium alloys. In *Essential readings in magnesium technology* (pp. 565-572). Springer, Cham.
- [29] Song, G.; Song, S. A possible biodegradable magnesium implant material. *Adv. Eng. Mater.* 2007, 9, 298–302.
- [30] Witte, F.; Hort, N.; Vogt, C.; Cohen, S.; Kainer, K.U.; Willumeit, R.; Feyerabend, F. Degradable biomaterials based on magnesium corrosion. *Curr. Opin. Solid State Mater. Sci.* 2008, 2, 63–72 .
- [31] Song, G.; Atrens, A. Understanding magnesium corrosion—A framework for improved alloy performance. *Adv. Eng. Mater.* 2003, 5, 837–858 .
- [32] Tian, P., Peng, F., Wang, D., & Liu, X. (2017). Corrosion behavior and cytocompatibility of fluoride-incorporated plasma electrolytic oxidation coating on biodegradable AZ31 alloy. *Regenerative biomaterials*, 4(1), 1-10.